

Received 25 May 2022, accepted 16 June 2022, date of publication 21 June 2022, date of current version 15 September 2022.

Digital Object Identifier 10.1109/ACCESS.2022.3184695

The Voltage Security Region Calculation Method of Receiving-End Power System Based on the Equivalence of Transient Process

BO LI¹, LINXUAN TIAN², XU LUO¹, FAN MOU³, WENGUO WU², XUAN FAN¹,
YUAN ZHU³, AND TAO NIU¹ , (Member, IEEE)

¹State Grid Chongqing Economic Research Institute, Chongqing 400044, China

²State Key Laboratory of Power Transmission Equipment and System Security, Chongqing University, Chongqing 400044, China

³State Grid Chongqing Electric Power Company, Chongqing 402160, China

Corresponding author: Tao Niu (niutthu@qq.com)

This work was supported by the 2021 Science and Technology Project 1# of State Grid Chongqing Electric Power Company.

ABSTRACT In order to ensure the voltage security of the receiving-end power grid under both steady state and N-1 faults, it is necessary to conduct an accurate dynamic reactive power reserve assessment to ensure its normal voltage operation range at steady state. In other words, it's to determine the power grid voltage security region which is a transient stability constrained optimal power flow (TSCOPF) problem essentially. However, it needs to consider a large amount operational snapshots and corresponding transient constraints under each snapshot, which increases the computational burden heavily. To overcome this issue, this paper proposes a calculation method for the voltage security region of receiving-end power grid through the equivalence of the transient process. Firstly, based on the power grid partition and the matrix of graph theory, the different snapshots are selected to obtain typical snapshots, and then for the typical snapshots sought, the transient stability constraints under the fault are transformed into steady-state constraints. In other words, the form is consistent with the steady-state equation but the impedance matrix parameters are equivalently adjusted. In essence, it is equally to replace the constraints of the optimization problem under the premise of ensuring that the consistency of the boundary conditions, so as to greatly accelerate the solution speed under the premise of ensuring the accuracy of the solution, and the calculation cases made in the modified IEEE9 system and the modified IEEE39 system prove the effectiveness and reliability of the proposed method in this paper.


INDEX TERMS The equivalence of transient process, voltage security region, receiving-end power system.

I. INTRODUCTION

With the development of China's economy and society, China's demand for various energy sources, especially power energy, is also increasing. In order to fully alleviate the shortage of power energy in the eastern region and promote the consumption of new energy in the western region, China has built a number of large-capacity and long-distance transmission lines based on "three crosses and four straights." However, the voltage security problems brought about by the "weak AC systems and strong HVDC" situation formed by the construction of such large-scale direct current transmission lines have become more prominent. To ensure

the safe operation of the grid at the receiving end, the security and stability of the grid voltage needs to be studied. The "point-by-point method" is a common approach when analyzing the security stability of the grid. The point-by-point method calculates the current operating conditions based on the grid parameters and the current operating state. Based on the grid parameters and the current operating state through tools such as power flow calculation, stability limitation calculation or transient simulation, the point-by-point method calculates state of the grid after a disturbance or fault occurs in a given state and judge whether the current operating state is "normal and safe" based on the calculation results.

The disadvantage of the point-by-point method is that it can only determine whether the current state is stable/secure based on the calculation results, but cannot give

The associate editor coordinating the review of this manuscript and approving it for publication was Amedeo Andreotti .

the stability/security margin intuitively. Compared to the point-by-point method, the voltage security region/stability region (VSR) method [1]–[4], which has been developed since the 1960s. It can more clearly and intuitively portray the security state of the power grid and directly give the current state of the grid security/stability. This enables the security and stability of the power system to be under the monitor of the dispatcher at all times. The visualization of the security region can provide sufficient information for the dispatch operators, which is helpful for the dispatch operators to have sufficient understanding of the security and stability of the grid during operation. Definition of the security region, i.e., the set of all operating points that can satisfy the corresponding constraints. When the grid topology parameters, the assuming faults/disturbances are given, the corresponding security regions are uniquely determined. When considering the system constraints of small interference stability, the literature [5] studied the approximate linear expression of the quiescent voltage stability region hyperplane that guarantees the static voltage stability of the system (i.e., the stability of the small interference voltage). When considering constraints such as large disturbances or system failures, the literature [6], [7] calculated dynamic security regions that guarantee proper operation after failure.

Methods for studying voltage security regions can be generally classified into two categories: fitting method and analytical methods. The fitting method is usually a way to obtain an approximate linear expression for the security region hyperplane by generating a large number of operating points based on a given network topology and device control parameters and using different fitting tools. In addition to traditional optimization methods such as least squares fitting, artificial neural network methods can be used to fit. For example, the literature [8] and [9] used artificial neural network methods to fit the static and dynamic (transient) security region boundaries, respectively. Although the fitting method is simple and convenient and can be used for different kinds of security regions and different types of systems, it still suffers from difficulties such as requiring a large number of calculations and inconvenient online applications. In particular, using artificial neural networks, when the inherent parameters of the power system change (e.g., the system topology changes due to planning), a large number of calculations need to be performed again. Compared with the proposed method, the analytical method has the advantages of clear physical meaning and theoretical interpretability. For the static security region, the analytical method generally approximates the expression of the security region hyperplane by linearizing the power flow; for the dynamic security region, the approximate expression of the security region boundary is obtained by linearizing the state equation and approximating the values of the state and algebraic variables after the fault occurs.

If voltage in the steady-state is not controlled before a fault within the voltage security region based on the assuming set of faults, once a fault occurs, the voltage

of the system will rapidly fall outside the security range, even leading to the voltage collapse of the power system. Therefore, pre-plan evaluate the dynamic reactive power reserve margin quickly and accurately before the fault occurs, and determine the voltage security operating range (VSR) of the N-1 fault to guarantee sufficient dynamic reactive power reserve in advance during steady-state operation are necessary to ensure the safe operation of the power grids. For the voltage security region, the literature [10] proposed a novel voltage security region calculation model for distribution network and analyzed the boundary of the voltage security region from multiple levels. In order to solve the contradiction between the computational efficiency and accuracy of the voltage security region, the literature [11] proposed a generalized optimization model of the voltage security region based on the topological characteristics of the voltage security boundary. For the wind farm and its system side, literature [12] proposed a robust voltage security region calculation method for VSC-HVDC. For large scale power systems with a high proportion of new energy penetration, calculating a reasonable voltage security region is an effective and promising method to prevent cascading failures of wind farms. Therefore, the literature [11] proposed a universal optimization model that can tracks the boundary of the voltage security region. To a certain extent, the balance between computational efficiency and computational accuracy was achieved. Aiming at the situation that the high proportion of distributed generators make the operation state of the distribution network too complex, the literature [13] proposed a hyperplane expression of the boundary of the static voltage security region of the complex power injection space. In order to deal with the difficulty of calculating the voltage security region in the gathering area of large-scale wind farms, the literature [14] proposed an autonomous voltage security region calculation method based on the step search algorithm, which realized the voltage security region calculation of each wind farm and the point of common coupling (PCC) substation. In order to solve the problem of random increase of load demand and mismatch of transmission line and generator structure in the future, the literature [15] applied artificial neural network to realize the online monitoring and controlling of system voltage security under various faults, which enhanced its flexibility.

And to solve the conservative issues and heavy computation burdens of the traditional method, the literature [16] proposed the concept of the autonomous-synergic voltage security region (AS-VSR) and corresponding dynamic constraint coefficient pruning (DCCP) computation method, which obtained accurate results in both linearized and nonlinearized robust optimization problems. And to avoid voltage collapse and operate more safely and reliably, literature [17] proposed a novel improved particle swarm optimization and recursive least square (IPSO-RLS) hybrid algorithm. It can optimize the active power and reactive power at the same time of getting the voltage security region.

As for the power system with direct current, a new concept of a fault security region (FSR) is proposed [18] based on the description of the active power and exchanged reactive power of inverter station. In this way, the subsequent commutation failure can be prevented under the condition that the effect of varying active power and reactive power of LCC-HVDC on power systems is balanced.

However, some challenges remain:

(1) There are a large amount of operational snapshots in the power system, and there is still not a unified and reliable method for how to select the typical snapshots that is most similar to operating snapshots of the actual system.

(2) The transient constraints of the original TSCOPF problem contains a large number of differential and algebraic equations, and the direct solution with electromechanical transient simulation software such as PSD-BPA has high computational complexity and long calculation time, which is difficult to meet the requirements of the scheduling time of 5 to 15 minutes in China's power system.

(3) In the traditional method, when dealing with transient constraints, the differential equation is differentiated into the original optimization problem, but the final solution is greatly affected by the step size. When the step size is small, the solution accuracy is higher, but the solution time is too long. However, when the step size is large, the solution accuracy is low, and sometimes it is difficult to meet the needs of normal dispatching of the power system.

Therefore, in order to solve the above challenges, this paper proposes a voltage security region calculation method suitable for power grids. The main contributions of this paper are as follows:

(1) First, for the situation that the complex power grids have many operational snapshots that are difficult to deal with directly, make preliminary adjustments and simplifications according to the geographical division of the power grid, then determine the basic snapshots based on the matrix of graph theory, and finally define the relevant indicators to screen out the key snapshots with small transmission margin and large transmission capacity.;

(2) Establish the original TSCOPF problem, simplify its complex transient constraints by transforming its original short-circuit fault into a permanent ground fault with constant ground impedance through the equivalent waveform of the dropping area. The basis of equivalence is to ensure the consistency of voltage security boundaries. After this, change different snapshots and solve the corresponding constant ground impedance value (critical impedance). And then use L-M fitting method to find the relationship and solve its analytical expressions between critical impedance and the initial operating state of the system, substitute it into the power flow equation to form equivalent transient constraints, and finally replace the transient constraints with them to solve the original optimization problem. The result of numerical cases analysis proves that the proposed method is more convenient than the traditional TSCOPF method, and it is effective and reasonable.

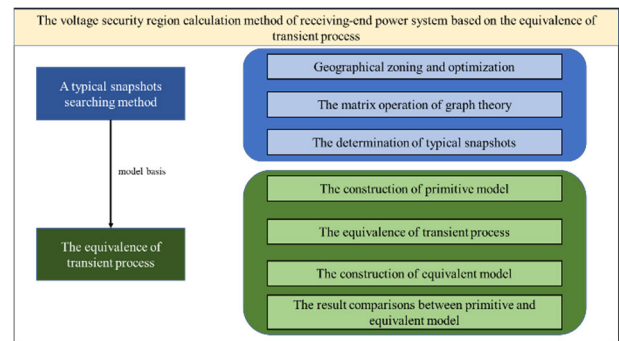


FIGURE 1. The research framework of this paper.

And the main contributions of this paper are as follows:

1) Firstly, optimize the end nodes to ensure the active power flow in the same direction between regions. Then by the matrix operation of graph theory, determine the typical snapshots.

2) Secondly, construct the primitive tscopf model based on the AC/DC power system. Then convert the equations of transient process into steady form which is similar to the equations of the power flow and construct equivalent model.

3) Finally, make a result comparison between primitive and equivalent model.

II. A TYPICAL SNAPSHOTS SEARCHING METHOD BASED ON THE POWER GRID GEOGRAPHIC PARTITIONING ALGORITHM AND THE MATRIX OF GRAPH THEORY

In this paper, aiming at solving the problems of a large number of nodes in the original power grid, complex topology and difficulty in real-time online monitoring, a typical snapshot searching method based on the grid geographic partitioning algorithm and the matrix of graph theory is proposed.

A. GEOGRAPHICAL ZONING AND OPTIMIZATION OF THE POWER GRID

The actual grid has a large number of nodes and a complex structure, which is difficult to analyze directly. Therefore, it needs to be partitioned according to the geographical attributes of the station, which means that nodes with the same location characteristics are divided into the same partition. However, this geographic division principle has some drawbacks when dealing with the boundary nodes of each partition, for example, the boundary nodes or end nodes will be divided into different partitions because of the long distance between them and the upstream nodes. Therefore, to address the limitations of the previous method, the end nodes can be further optimized. When the end nodes are only connected to their parent nodes, the end nodes are shrunk to the partition where the parent nodes are located, and when the parent nodes are dendritic nodes, the shrinkage continues to ensure that the active power flow in the same direction between regions. And the flow chart are as follows:

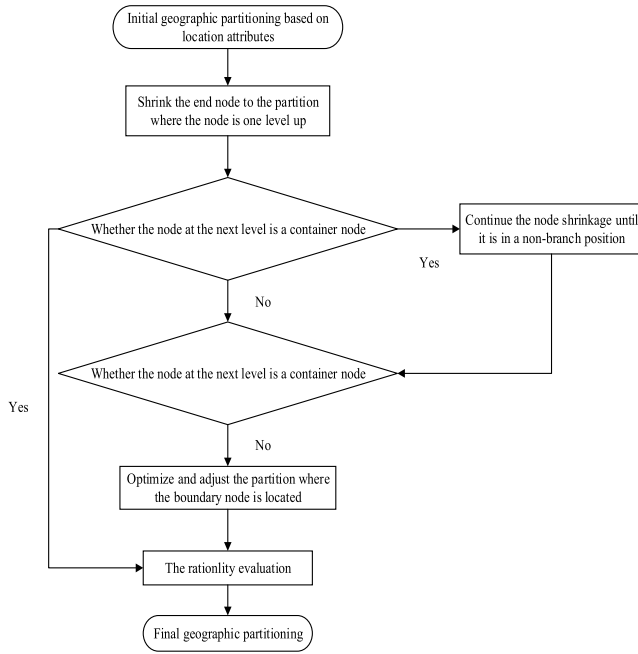


FIGURE 2. Partition optimization flowchart.

B. TYPICAL TRANSMISSION SNAPSHOTS DETERMINATION BASED ON THE MATRIX OF GRAPH THEORY OPERATION

Based on the above optimization and adjustment of the geographical partition, we need to search for transmission snapshots composed of corresponding lines and determine typical snapshots by commutating the security margin. According to the relevant principles of graph theory and the characteristics of the transmission snapshots, above questions are converted to search for the minimum cut set of the power grid partition topology graph. And the steps in Table 1 aim to convert the power grid partition topology graph into the adjacency matrix and then the path matrix, finally search for the transmission snapshots by a series of matrix operations. And the specific operation steps are as follows:

C. DETERMINATION OF TYPICAL SNAPSHOTS

After the n basic snapshots are determined earlier, the snapshots with large transmission capacity and small security margin can continue to be filtered out as typical snapshots, and the screening steps are as follows:

First, the current flow of the *i*th snapshot of the system is normalized:

$$P'_i = \frac{p_i - \min\{P_j\}}{\max\{P_j\} - \min\{P_j\}} \quad j = 1, 2, \dots, n \quad (1)$$

Let the limit transmission power of the *i*th snapshot be P_i^{\max} and then the transmission capacity margin of the snapshot is M_i .

$$M_i = \frac{P_i^{\max} - P_i}{P_i^{\max}} \quad (2)$$

TABLE 1. Flowchart of a typical transmission snapshot.

STEP1	According to the previously obtained grid partition topology diagram, write out its adjacency matrix A, assuming that there are n partitions, then A is n *n square matrix, when there is a direct connection between the two partitions, the corresponding value is 1, and when there is no direct connection, the corresponding value is 0
STEP2	Find the path matrix P step1: Initialize the path matrix P=A; step2:j=1; step3:if $p_{ij} = 1$ For k=1:n $p_{ik} = p_{ik} p_{jk}$ end end step4:i=i+1 if $i \leq n$ go to step3 end step5:j=j+1 if $j \leq n$ go to step2 end
STEP3	Calculate the upstream transmission matrix $Q = P + I$
STEP4	Calculate the downstream power matrix \bar{Q}
STEP5	Calculates the power delivery matrix $S_k = Q_k \bar{Q}_k^T$
STEP6	Calculate the transmission cross-snapshots matrix $T = S_k \&$

A

As the heavier the snapshot of power flow, the smaller the security margin, the greater the importance of the corresponding snapshot, so the importance of the snapshot index can be defined as follows.

$$I_i = P'_i - 1n(M_i) \quad (3)$$

III. PRIMITIVE AND EQUIVALENT MODELS FOR TRANSIENT PROCESSES

After screening out the critical snapshots according to the snapshot importance index, the next step can be the calculation of the voltage security region of each bus under the critical snapshot. To solve the voltage security region under N-1 faults at a certain snapshot, it is essential to solve a TSCOPF (Transient Stability Constrained Optimal Power Flow) problem, which is first explained in its specific form as follows.

For a complicate AC power system, the specific model used and its equations are as follows.

a) The generator is used in the four-order model as follows:

$$\dot{\delta} = 2\pi f (\omega - \omega_0) \quad (4)$$

$$\dot{\omega} = \frac{1}{M} (P_m - P_e - D(\omega - 1)) \quad (5)$$

$$\dot{E}'_q = \frac{1}{T'_{d0}} (V_f - E'_q - (X_d - X'_d) I_d) \quad (6)$$

$$\dot{E}'_d = \frac{1}{T'_{q0}} (-E'_d - (X_q - X'_q) I_q) \quad (7)$$

In the above model, $\dot{\delta}$ means the derivative of power angle of the generator, f means the frequency of the power system, ω and ω_0 means the angular frequency and its reference value of the generator. $\dot{\omega}$ means the derivative of angular frequency of the generator, P_m means mechanical torque, P_e means electromagnet tongue, D means the damping coefficient of power, \dot{E}'_q means the derivative of quadrature axis transient potential, \dot{E}'_d means the derivative of direct axis transient potential.

b) The AVR is used in the model as follows:

$$\dot{V}_m = \frac{1}{T_r} (V - V_m) \tag{8}$$

$$\dot{V}_{rx} = \frac{1}{T_a} \left(K_a \left(V_{ref} - V_m - V_{ry} - \frac{K_f}{T_f} V_f \right) - V_{rx} \right) \tag{9}$$

$$\dot{V}_{ry} = -\frac{1}{T_f} \left(\frac{K_f}{T_f} V_f + V_{ry} \right) \tag{10}$$

$$\dot{V}_r = \begin{cases} V_{rx}, & (V_r \min \leq V_{rx} \leq V_r \max) \\ V_r \max, & (V_{rx} \leq V_r \min) \\ V_r \min, & (V_{rx} \geq V_r \max) \end{cases} \tag{11}$$

$$\dot{V}_f = -\frac{1}{T_e} (V_f (1 + S_e (V_f)) - V_r) \tag{12}$$

$$P = VI_d \sin(\delta - \theta) + VI_q \cos(\delta - \theta) \tag{13}$$

$$Q = VI_d \cos(\delta - \theta) - VI_q \sin(\delta - \theta) \tag{14}$$

$$E'_q = V \cos(\delta - \theta) + R_a I_q + (X_d - X'_d) I_d \tag{15}$$

$$E'_d = V \sin(\delta - \theta) + R_a I_d - (X_q - X'_q) I_d \tag{16}$$

In the above model, δ means the power angle of the generator, I_d means the current of direct axis, I_q means the current of quadrature axis, R_a means the resistance of the armature winding, X_d means the direct axis reactance, X'_d means the direct axis transient reactance, X_q means the quadrature axis reactance, X'_q means quadrature axis transient reactance.

c) The load is used in the model as follows:

$$P = VI_r \sin \theta + VI_m \cos \theta \tag{17}$$

$$Q = VI_r \cos \theta - VI_m \sin \theta \tag{18}$$

$$V \sin \theta + E'_r = X' I_m - R_s I_r \tag{19}$$

$$V \cos \theta + E'_m = -X' I_r - R_s I_m \tag{20}$$

In the above model, X' means transient reactance, the parameters with subscript r means rotor-related parameters, the parameters with subscript m means parameters related to iron loss and the parameters with subscript s means stator-related parameters.

The above is a model for a purely AC system, if there is DC feeding in the power system, the following model needs to be added.

d) The detailed control system of HVDC are as follows.

$$I_{DC}^{od} = \begin{cases} I_{DC0}^{od}, & (V_{DC} \geq V_{DC}^{th1}) \\ I_{DC0}^{od} - K_D (V_{DC} - V_{DC}^{th1}), & (V_{DC}^{th1} < V_{DC} < V_{DC}^{th2}) \\ I_{DC \min}^{od}, & (V_{DC} \leq V_{DC}^{th2}) \end{cases}, \tag{21}$$

$$(V_{DC}^{th2} \leq V_{DC} \leq V_{DC}^{th1})$$

$$\cos \gamma_0 = \frac{\sqrt{2}\pi X_C I_{DC}}{3T_{DC} V_{CS}} + \cos \beta_b \tag{22}$$

$$\cos \gamma = \frac{\sqrt{2}\pi X_C I_{DC}^{od}}{3T_{DC} V_{CS}} + \cos \beta_a \tag{23}$$

In the above model, K_D means gain coefficient, γ means extinction angle, β means conduction angle.

$$V_{DC} = \frac{3\sqrt{2}}{\pi} T_{DC} V_{CS} \cos\left(\gamma + \frac{\mu}{2}\right) \cos \frac{\mu}{2} \tag{24}$$

$$I_{DC} = \frac{\sqrt{2}}{\omega X_C} V_{CS} \sin\left(\gamma + \frac{\mu}{2}\right) \sin \frac{\mu}{2} \tag{25}$$

$$P_{DC} = \frac{3}{\pi \omega X_C} V_{DC}^2 \sin(2\gamma + \mu) \sin \mu \tag{26}$$

$$Q_{DC} = P_{DC} \tan \varphi, \quad \cos \varphi = \cos\left(\gamma + \frac{\mu}{2}\right) \cos \frac{\mu}{2} \tag{27}$$

$$\Rightarrow F_{DC,i}^0 (V_{DC,i}, V_{CS,i}, Q_{DC,i}, P_{DC,i}, \gamma_i, \mu_i, \varphi_i, I_{DC,i}) = 0 \tag{28}$$

In the above model, V_{DC} means the DC voltage, I_{DC} means the DC current, P_{DC} means the direct active power, Q_{DC} means the direct reactive power, φ means the power factor, and μ means the angle of commutation, γ means extinction angle.

With the above model, the optimization problem shown in the following equation can be established(29, 31).If direct current exists, the optimization can be summarized as 29, 30 and 31.

$$\max_{\Delta Q_g} \sum_{i=1}^N (U_i^{0,\max} - U_i^{0,\min})$$

$$s.t. P_{Gi} - P_{Li} = U_i \sum_{j=1}^{j=n} U_j (G_{ij} \cos \delta_{ij} + B_{ij} \sin \delta_{ij})$$

$$Q_{Gi} - Q_{Li} = U_i \sum_{j=1}^{j=n} U_j (G_{ij} \sin \delta_{ij} - B_{ij} \cos \delta_{ij})$$

$$P_{Gi \min} \leq P_{Gi} \leq P_{Gi \max}, \quad Q_{Gi \min} \leq Q_{Gi} \leq Q_{Gi \max}$$

$$U_{i \min} \leq U_i \leq U_{i \max}$$

$$|\delta_i - \delta_j| < |\delta_i - \delta_j|_{\max} \tag{29}$$

$$F_{DC,i}^0 (V_{DC,i}, V_{CS,i}, Q_{DC,i}, P_{DC,i}, \gamma_i, \mu_i, \varphi_i, I_{DC,i}) = 0$$

$$\underline{\gamma}_i \leq \gamma_i \leq \bar{\gamma}_i,$$

$$\underline{\mu}_i \leq \mu_i,$$

$$\underline{V}_{CS,i} \leq V_{CS,i} \leq \bar{V}_{CS,i}$$

$$\underline{Q}_{DC,i} \leq Q_{DC,i} \leq \bar{Q}_{DC,i} \tag{30}$$

$$\dot{x} = f(x, y, u)$$

$$0 = g(x, y, u) \tag{31}$$

However, if the original optimization problem is solved directly, the computational model is complex and the solution time is long, which is difficult to meet the requirements of the actual power system for the speed of the voltage security region's calculation. Therefore, we consider converting the original TSCOPF problem into a SCOPF(Stability

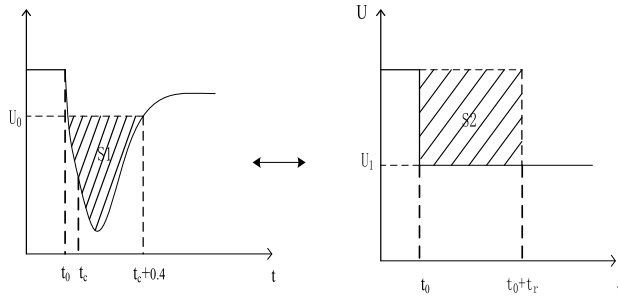


FIGURE 3. Transient isometric procedures.

Constrained Optimal Power Flow) problem, converting the complex differential and algebraic equations constraints in transient state into a steady-state constraint (the same form as constraints of the steady-state power flow and constraints of variable upper and lower limits, but with different physical meaning), and converting the original transient fault into an equivalent permanent ground fault under the premise of ensuring the same boundary conditions of the voltage security region, thus greatly speeding up the solution speed while ensuring certain accuracy. It is simplified as the concrete form as follows.

$$\max_{\Delta Q_g} \sum_{i=1}^N (U_i^{0,\max} - U_i^{0,\min}) \quad (29), (30)$$

$$Z = R + jX = f(P^0, Q^0, V^0) \quad (32)$$

As shown in the above figure, the left figure is the voltage waveform in the transient process, U_0 is the minimum voltage allowed in the system specific time after fault removal. According to relevant standards, for the voltage 0.4s after fault removal, this value is generally taken as 0.85. Set short-circuit faults to the system and adjust its related parameters until the voltage just reaches 0.85 after fault clearing. Write down the voltage dropping area S_1 at this time as the boundary conditions, as shown in the above figure 3.

Next step is to change nodal admittance matrix corresponding to the location of the original system fault to keep equivalent with the original fault. In fact, it is to set the permanent ground fault and change the ground impedance until the voltage dropping area S_2 is equivalent to the mentioned fault to reach the same boundary conditions, as shown in formula (31). And the waveform on the right side of Figure 3 is an ideal model, which is based on the assumptions that the initial value after the voltage dropping is equal to its steady-state value (idealized processing, the actual fluctuation is very small). According to different degrees of system strength and weakness as well as the different configuration of each component parameter within the system, the dropping area can be defined differently, and the way it is defined in this paper is shown in figure 3. According to a number of fault simulations and related standards in the power system, we can compute S_2 according to the location, the lasting time of the fault and S_1 mentioned

TABLE 2. L-M data fitting algorithm steps.

Input: A vector function $f: R^m \rightarrow R^n$ with $n \geq m$, a measurement vector $x \in R^n$ and an initial parameters estimate $p_0 \in R^m$.
Output: A vector $p^+ \in R^m$ minimizing $\ x - f(p)\ ^2$.
Algorithm:
$k:=0; v:=0; p:=p_0;$
$A:=J^T J; \epsilon_p := x - f(p); g := J^T \epsilon_p;$
Stop: $(\ g\ _\infty \leq \epsilon_1); \mu := \tau * \max_{i=1, \dots, m} A(i, i);$
While(not loop) and ($k < k_{max}$)
$K:=k+1;$
Repeat
Solve $(A + \mu I)\delta_p = g;$
If $(\ \delta_p\ \leq \epsilon_2 \text{ or } \ p\)$
Stop:=true;
Else
$p_{new} := p + \delta_p;$
$\rho := (\ \epsilon_p\ ^2 - \ x - f(p_{new})\ ^2) / (\delta_p^T (\mu \delta_p + g));$
If $\rho > 0$
$p = p_{new};$
$A := J^T J; \epsilon_p := x - f(p); g := J^T \epsilon_p;$
Stop: $(\ g\ _\infty \leq \epsilon_1) \text{ or } (\ \epsilon_p\ ^2 \leq \epsilon_3);$
$\mu := \mu * \max(\frac{1}{3}, 1 - (2\rho - 1)^3); v := 2;$
Else
$\mu := \mu * v; v := 2 * v;$
End if
End if
Until $\rho > 0$ or (stop)
End while
$p^+ := p;$

above, etc. After the calculation is completed, we can determine the equivalent failure lasting time t_r and in this paper we set the value of t_r is 0.4~0.5 s according to the severity of the fault. After getting S_2 and t_r , we can get the critical voltage U_1 by S_2 divided by t_r , as shown in formula (31). And this step achieves to calculate the voltage dropping areas in normal transient process and then transform it into the voltage dropping area in equivalent transient process. Finally, we can get U_1 as the reference for the severity of permanent ground fault.

After getting the critical voltage U_1 corresponding to the permanent ground fault, change the grounding impedance for simulation at the same fault location and continuously adjust the value of the grounding impedance until the corresponding buses' voltage reach the critical voltage, write down the value of the grounding impedance at this time as the critical impedance, change the system operating state so that it runs on different typical snapshots, we can get different values of the critical impedance.

$$S_2 = f(S_1) \Rightarrow U_1 = \frac{S_2}{t_r} \quad (33)$$

$$Z = R + jX = g(P^0, Q^0, V^0) \quad (34)$$

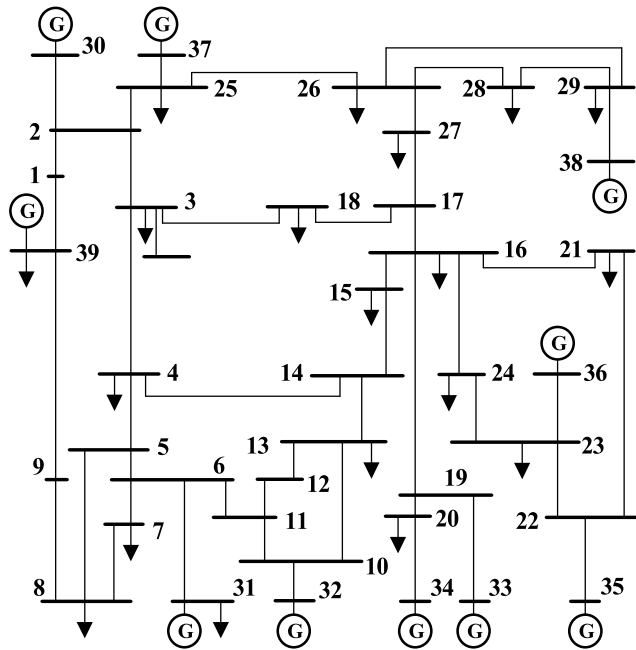


FIGURE 4. Modified IEEE 39 node system.

TABLE 3. Detailed fault information of modified IEEE39 system.

Information	modified IEEE 39 system
Occurrence time/s	1.5
Clearing time/s	1.6
Grounding resistance / Ω	0.00001
Bus voltage U_0 in transient process/p.u.	0.8560
Bus voltage U_1 in equivalent process/p.u.	0.9834

TABLE 4. Critical impedance matrix (Q1, Q2, Q3 are the reactive power output of three typical reactive devices selected).

Critical impedance(Ω)	Q1(Mvar)	Q2(Mvar)	Q3(Mvar)
9.92+0.1j	0	0	0
8.76+0.1j	20	20	20
8.29+0.1j	40	40	40
7.87+0.1j	60	60	60
7.49+0.1j	80	80	80
7.15+0.1j	100	100	100
6.84+0.1j	120	120	120
6.55+0.1j	140	140	140
6.29+0.1j	160	160	160
6.04+0.1j	180	180	180

To obtain the approximate quantitative relationship between the critical impedance and each control variable in the steady-state operation of the system, the L-M data fitting algorithm is used to process the obtained data. The specific steps are shown below.

IV. CASE STUDY

Case 1: In order to verify the accuracy and feasibility of the proposed method, it was verified by modified the IEEE39

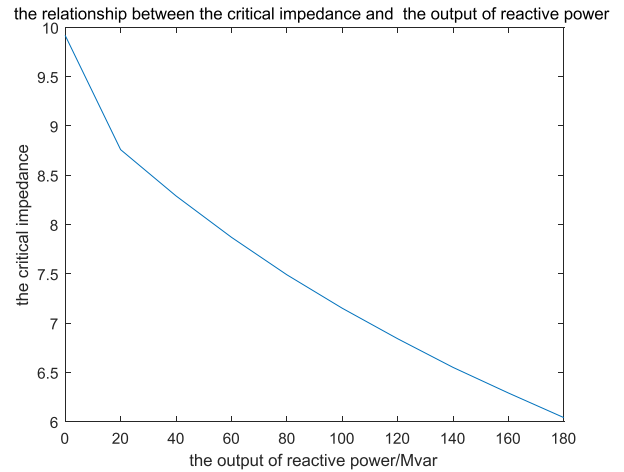


FIGURE 5. The relationship between the critical impedance and the output of reactive power.

TABLE 5. Comparison of voltage security region calculation results before and after transient equivalence of PV nodes of IEEE39 system under a typical snapshot.

Information	Transient simulation	Transient equivalence
Bus30	[0.973,1.032]	[0.9755,1.0298]
Bus32	[0.968,1.029]	[0.9708,1.0256]
Bus33	[0.979,1.024]	[0.9815,1.0198]
Bus34	[0.988,1.031]	[0.9908,1.0302]
Bus35	[0.982,1.055]	[0.9855,1.0492]
Bus36	[1.013,1.075]	[1.0185,1.0698]
Bus37	[1.015,1.054]	[1.0182,1.0495]
Bus38	[1.005,1.034]	[1.0086,1.0288]
Bus39	[1.013,1.058]	[1.0187,1.0496]
The comparison of time	4.585s	1.842s

test system, in which the topology is shown in Figure 4 and its specific fault parameters are shown in Table 3.

As can be seen from the above figure, the computation of voltage security region after transient equivalence is significantly faster compared with the direct transient simulation, and the overall error is still within an acceptable range, although the calculation results are conservative.

For different typical snapshots, the above figure shows the error of the given calculation method. In Figure 7, we can conclude that the calculation method is greatly influenced by the kind of snapshots and there are much difference between low limit and high limit.

Case 2: For the power system with direct current, it was verified by modified IEEE9 test system, in which the topology is shown in Figure 8 and its specific fault parameters are shown in Table 6 and its specific parameters are shown in Table 7.

Figure 9 shows the comparisons of the voltage security region computation results in two different ways for the modified IEEE9 system. In this figure, the solid lines

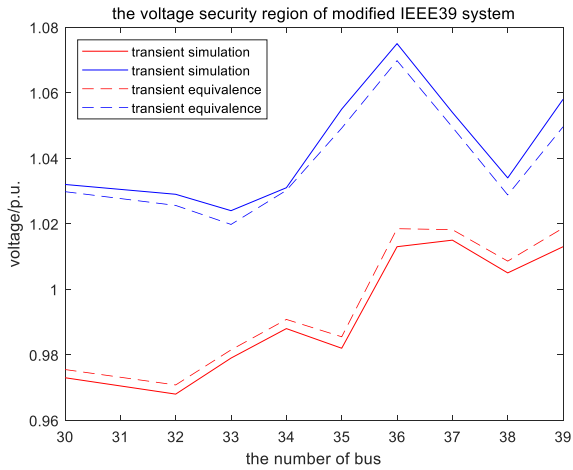


FIGURE 6. The voltage security region of modified IEEE39 system.

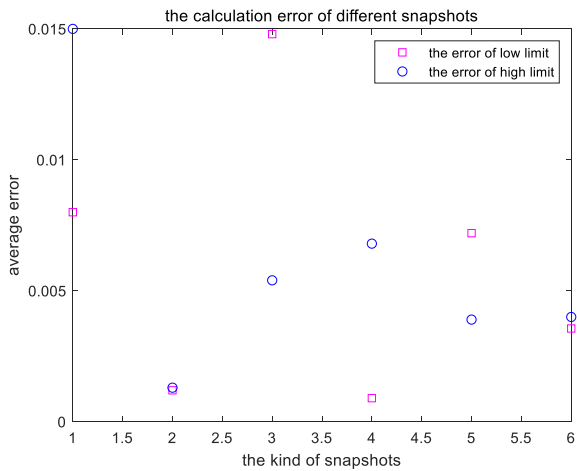


FIGURE 7. The calculation error of different snapshots in modified IEEE39 system.

TABLE 6. Detailed fault information of modified IEEE9 system.

Information	modified IEEE 9 system
Occurrence time/s	1.5
Clearing time/s	1.6
Grounding resistance / Ω	0.00001
Bus voltage U_0 in transient process/p.u.	0.8506
Bus voltage U_1 in equivalent process/p.u.	0.9512

represent the voltage security region in transient simulation and the dashed lines represent the voltage security region in transient equivalence method previously mentioned. What is more, the blue line means the upper limit of the voltage security region and the red line means the lower limit of the voltage security region. The comparisons between the two different ways indicate the accuracy of the proposed method.

For the modified IEEE 9 system with double-infeed DC, the result of voltage security region in transient simulation

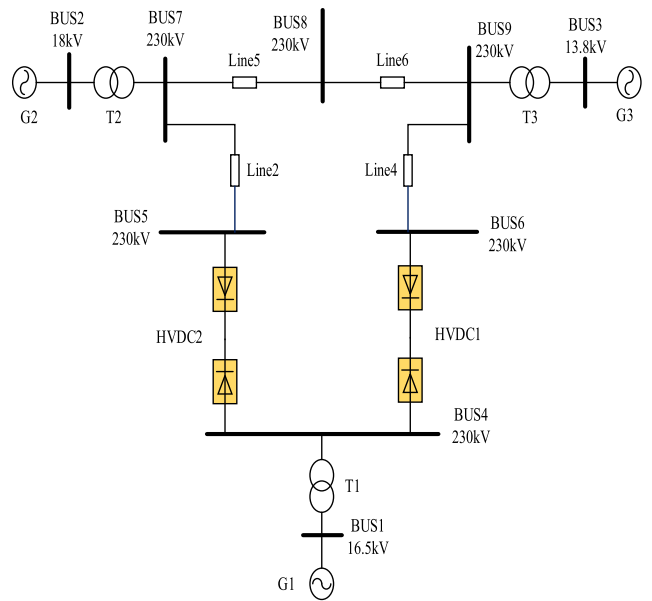


FIGURE 8. Modified IEEE9 system.

TABLE 7. The parameters of IEEE 9 double-infeed HVDC test system.

The parameters of IEEE 9 double-infeed hvdc test system						
The rectifier-end	T_{rc}	K_r	T_r	V_D^m	I_D^m	α^{\min}
	0.005	0.10	0.02	0.4	0.5	5°
The inverter-end	T_{ic}	K_{i1}	T_{i1}	K_{i2}	T_{i2}	β_{\min}
	0.005	0.10	0.02	0.10	0.02	90°

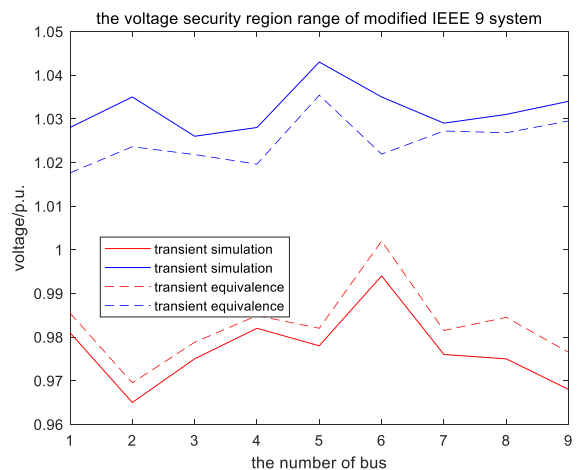


FIGURE 9. The voltage security region of modified IEEE9 system.

and transient simulation are shown in Figure 7. We can conclude that the error between transient simulation and transient equivalence is no more than 0.01.

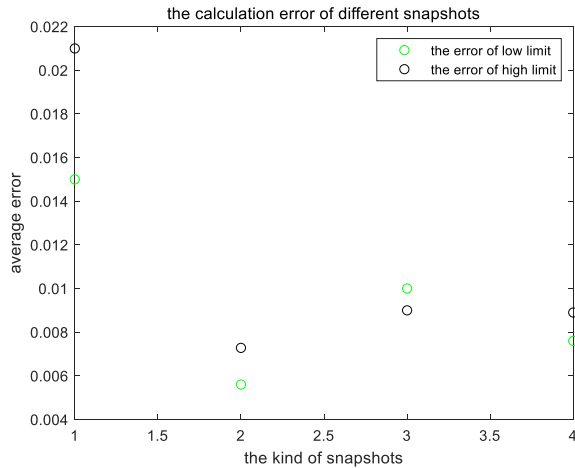


FIGURE 10. The calculation error of different snapshots.

For different typical snapshots, the above figure shows the error of the given calculation method. In Figure 10, we can conclude that the calculation method is greatly influenced by the kind of snapshots.

V. CONCLUSION

In order to overcome the problems of a large number of differential equations, high computational complexity and long computation time in the traditional solution method of TSCOPF problem, this paper proposes a method of calculating the voltage security region of power grid based on transient process equivalence, including the typical snapshot searching method based on grid geographic partitioning algorithm and graph theory matrix and the voltage security region calculation method based on transient process equivalence. On the one hand, the typical snapshots with large operating capacity and low security region can be screened out from a large number of snapshots, and then the complex differential equations in the transient process can be converted into algebraic equations similar to the power flow equations on the basis of boundary equivalence for the screened typical snapshots, and then the relationship between the critical impedance and the system operating state can be expressed in analytical form by L-M fitting method, and the original transient equations can be replaced by similar power flow equations. The validity and reliability of the proposed method can be proved by solving the voltage security region problem before and after the simplification. From the final calculation results, it can be concluded that:

1) The calculation results of the voltage security region after transient equivalence are within the allowable range of errors and take less time.

2) However, the calculation range of the voltage security region after transient equivalence is smaller and the calculation results are more conservative, which may be caused by certain errors in the fitting process of the critical impedance and reactive power output of reactive equipment, or may be caused by certain rounding errors in the calculation

of the critical impedance in the transient process. What's more, it may have relationships with different operational snapshots.

3) For the modified IEEE9 system and the modified IEEE39 system, we can conclude that the range of voltage security region in transient equivalence is smaller than that in transient simulation. And the modified IEEE39 system is purely an AC system and the factors that need to consider are less than that in hybrid AC-DC systems, which results in smaller errors to a certain extent.

In future studies, the relationship between the error of the voltage security region calculation result and the different errors and operational snapshots will be considered, so as to further optimize the solution accuracy.

REFERENCES

- [1] R. Fishcl and J. A. De Maio, "Fast identification of the steady-state security regions for power system security enhancement," in *Proc. IEEE PES Winter Meeting*, Jan. 1976.
- [2] M. H. Banakar, F. D. Galiana, and J. Jarjis, "Security region in power network," in *Proc. IEEE Int. Symp. Circuits Syst.*, Dec. 1981, pp. 11–13.
- [3] J. Jarjis and F. D. Galiana, "Quantitative analysis of steady state stability in power networks," *IEEE Trans. Power App. Syst.*, vols. PAS-100, no. 1, pp. 318–326, Jan. 1981.
- [4] M. H. Banakar and F. D. Galiana, "Power system security corridors concept and computation," *IEEE Trans. Power App. Syst.*, vols. PAS-100, no. 11, pp. 4524–4532, Nov. 1981.
- [5] H. Li et al., "Practical boundary of static voltage stability domain on cut set power space," *Power Syst. Automat.*, vol. 29, no. 4, pp. 18–23, 2005.
- [6] Y. Zeng, "Practical dynamic safety domain for large power systems," *Automat. Electr. Power Syst.*, vol. 25, no. 16, pp. 6–10, 2001.
- [7] Y. Yu and J. Lin, "Practical analytical representation of dynamic safety domain boundary of power system," *J. Tianjin Univ., Dept. Natural Sci. Sci. Eng. Technol. Ed.*, vol. 30, no. 1, pp. 1–8, 1997.
- [8] C. Luo, H. Sun, and G. Xu, "Application of artificial neural networks in static safety domain analysis of power systems," *Power Syst. Automat.*, vol. 18, no. 2, pp. 13–18, 1994.
- [9] F. Z. Wang, Y. Z. He, and D. S. Chen, "Transient safety domain estimation for power systems based on artificial neural networks," *Power Syst. Automat.*, vol. 17, no. 4, pp. 17–22, 1993.
- [10] Q. Cai, Y. Li, C. Lin, Y. Li, K. Xiang, X. Huang, N. Zheng, and S. Guo, "Fast security analysis for urban power system based on full voltage level security region," in *Proc. IEEE 4th Conf. Energy Internet Energy Syst. Integr. (EI)*, Oct. 2020, pp. 215–220.
- [11] X. Li, T. Jiang, L. Bai, X. Kou, and F. Li, "A general optimization model for tracking voltage security region boundary in bulk power grids," *CSEE J. Power Energy Syst.*, vol. 8, no. 2, pp. 476–487, Aug. 2020.
- [12] T. Niu, F. Jiang, Q. Guo, Z. Wang, H. Ge, H. Jin, and B. Wang, "Robust voltage security regions with VSC-HVDC connections," in *Proc. IEEE Innov. Smart Grid Technol. Asia (ISGT Asia)*, May 2019, pp. 1450–1454.
- [13] T. Yang and Y. Yu, "Static voltage security region-based coordinated voltage control in smart distribution grids," *IEEE Trans. Smart Grid*, vol. 9, no. 6, pp. 5494–5502, Nov. 2018.
- [14] T. Niu, Q. Guo, H. Sun, Q. Wu, B. Zhang, and T. Ding, "Autonomous voltage security regions to prevent cascading trip faults in wind turbine generators," *IEEE Trans. Sustain. Energy*, vol. 7, no. 3, pp. 1306–1316, Jul. 2016.
- [15] K. Chakraborty and G. Saha, "Off-line voltage security assessment of power transmission systems using UVSI through artificial neural network," in *Proc. Int. Conf. Intell. Control Power Instrum. (ICICPI)*, Oct. 2016, pp. 158–162.
- [16] F. Li, T. Niu, L. Xue, Y. Li, T. Huang, and Z. Wu, "Autonomous-synergic voltage security regions in bulk power systems," *J. Mod. Power Syst. Clean Energy*, early access, Feb. 22, 2022.

- [17] S. Maihemuti, W. Wang, H. Wang, and J. Wu, "Voltage security operation region calculation based on improved particle swarm optimization and recursive least square hybrid algorithm," *J. Modern Power Syst. Clean Energy*, vol. 9, no. 1, pp. 138–147, 2021.
- [18] J. Ouyang, M. Pang, Z. Zhang, and J. Yu, "Fault security region modeling and adaptive current control method for the inverter station of DC transmission system," *IEEE Trans. Power Del.*, early access, Apr. 5, 2022, doi: 10.1109/TPWRD.2022.3164883.

BO LI is currently an Engineer with the State Grid Chongqing Economic Research Institute. His current research interest includes power system planning.

LINXUAN TIAN received the B.S. degree in electrical engineering from the Taiyuan University of Technology, Taiyuan, China, in 2021. He is currently pursuing the master's degree with the School of Electrical Engineering, Chongqing University. His current research interest includes dynamic reactive power reserve assessment of the power systems.

XU LUO is currently a Senior Engineer with the State Grid Chongqing Economic Research Institute. His current research interest includes power system planning.

FAN MOU is currently a Senior Engineer with State Grid Chongqing Electric Power Company. His current research interest includes power system planning.

WENGUO WU received the B.S. degree in electrical engineering from the China University of Mining and Technology, China, in 2021. He is currently pursuing the master's degree with the School of Electrical Engineering, Chongqing University. His current research interest includes dynamic reactive power reserve assessment of the power systems.

XUAN FAN is currently a Senior Engineer with the State Grid Chongqing Economic Research Institute. Her current research interest includes power system planning.

YUAN ZHU is currently a Senior Engineer with State Grid Chongqing Electric Power Company. His current research interest includes power system planning.

TAO NIU (Member, IEEE) received the B.S. and Ph.D. degrees from the Department of Electrical Engineering, Tsinghua University, Beijing, China, in 2014 and 2019, respectively. He is currently an Assistant Professor with Chongqing University, Chongqing, China. His research interests include power system operation and optimization, power system reliability assessment, voltage security region, automatic reactive power voltage control, and renewable generation integration and reactive power analysis of hybrid AC/DC systems.

...